Research
A SCIENCE PARTNER JOURNAL

RESEARCH ARTICLE

Long-Range Azimuthal Correlation, Entanglement, and Bell Inequality Violation by Spinning Gluons at the Large Hadron Collider

Yuxun Guo[1*], Xiaohui Liu[2,3*], Feng Yuan[1,4*], and Hua Xing Zhu[5,6*]

[1]Nuclear Science Division, Lawrence Berkeley National Laboratory, Berkeley, CA 94720, USA. [2]Center of Advanced Quantum Studies, School of Physics and Astronomy, Beijing Normal University, Beijing 100875, China. [3]Key Laboratory of Multi-scale Spin Physics, Ministry of Education, Beijing Normal University, Beijing 100875, China. [4]Institute for Theoretical Physics, Universität Tübingen, D-72076 Tübingen, Germany. [5]School of Physics, Peking University, Beijing 100871, China. [6]Center for High Energy Physics, Peking University, Beijing 100871, China.

*Address correspondence to: yuxunguo@lbl.gov (Y.G.); xiliu@bnu.edu.cn (X.L.); fyuan@lbl.gov (F.Y.); zhuhx@pku.edu.cn (H.X.Z.)

Citation: Guo Y, Liu X, Yuan F, Zhu HX. Long-Range Azimuthal Correlation, Entanglement, and Bell Inequality Violation by Spinning Gluons at the Large Hadron Collider. *Research* 2025;8:Article 0552. https://doi.org/10.34133/research.0552

Submitted 23 September 2024
Revised 10 November 2024
Accepted 23 November 2024
Published 5 February 2025

We apply the recently developed concept of the nucleon energy–energy correlator (NEEC) for the gluon sector to investigate the long-range azimuthal angular correlations in proton–proton collisions at the Large Hadron Collider. The spinning gluon in these collisions will introduce substantial nonzero $\cos(2\phi)$ asymmetries in both Higgs boson and top quark pair productions, where ϕ is the azimuthal angle between the forward and backward energy correlators in the NEEC observables. The genesis of the $\cos(2\phi)$ correlation lies in the intricate quantum entanglement. Owing to the substantial $\cos(2\phi)$ effect, the NEEC observable in Higgs boson and $t\bar{t}$ production emerges as a pivotal avenue for delving into quantum entanglement and scrutinizing the Bell inequality at high-energy colliders.

Introduction

Long-range correlation in particle productions in proton–proton (pp) collisions at the Large Hadron Collider (LHC) has attracted great attention in the last decade with tremendous efforts from both experiment and theory sides [1–4]. In this paper, we investigate this physics from a different perspective, applying the nucleon energy–energy correlator (NEEC) [5–7] at the LHC. We will show that the spinning gluon distribution in this framework [7] leads to sizable $\cos(2\phi)$ azimuthal asymmetries in forward–backward energy correlators in pp collisions, where ϕ is the azimuthal angle difference between these two energy correlators. These long-range $\cos(2\phi)$ asymmetries are signatures of the quantum entanglement, thereby providing the first test of the Bell inequality [8,9] within the entangled gluon system. Pursuing such a test in the Standard Model (SM) of particle physics at high-energy colliders has been very active in recent years [10–33]. In particular, exciting observations of quantum entanglement in top quark pair production in pp collisions at the LHC have been reported by the ATLAS and CMS collaborations [34–36].

The NEEC was introduced by Liu and Zhu [5] as a new method to explore the nucleon structures. It employs an asymptotic energy flow operator $\widehat{\mathcal{E}}(\theta_a)$, which measures energy deposits in the detector at a fixed angle θ_a relative to the nucleon incoming beam direction in collider experiments. Previous studies mainly focused on deep inelastic scattering [5–7,37], which will be explored at the future electron–ion collider [38–40]. In the following, we will study the NEEC observables in pp collisions. The comparison between these two collision systems will provide an opportunity to test the universality of NEECs. Meanwhile, the novel phenomena unveiled below will stimulate further experimental investigations and help decipher the origin of nearside ridges in pp collisions.

To investigate the NEEC at the LHC, we propose to measure the energy deposits along the beam directions of incoming hadrons with polar angles $\theta_{a,b}$ and azimuthal angles $\phi_{a,b}$, respectively; see the illustration in Fig. 1. The hard partonic scattering produces, e.g., the Higgs boson or top quark pairs. The experiment can be carried out by a coincidence measurement between the forward/backward energy flows and the hard interactions in the center. Because θ_a and θ_b are either small or close to π and in opposite directions, their rapidity difference will be large, for which we refer to as a long-range correlation. Meanwhile, we will show that different processes lead to different $\cos(2\phi)$ asymmetries. In particular, we find that the asymmetries in Higgs boson and top quark pair productions are quite sizable but with opposite signs. Therefore, a detailed study of these correlations will open a new avenue for precision SM physics.

In the following, we focus on the gluon NEEC [7]:

$$\begin{aligned} f^{\alpha\beta}_{g,\mathrm{EEC}}(x,\vec{n}_a) &= \int \frac{dy^-}{2\pi x P^+} e^{-ixP^+y^-} \\ &\times \left\langle P|\mathcal{F}^{+\alpha}(y^-)\mathcal{L}^\dagger[\infty,y^-]\widehat{\mathcal{E}}(\vec{n}_a)\mathcal{L}[\infty,0]\mathcal{F}^{+\beta}(0)|P\right\rangle \\ &= \left(-g_T^{\alpha\beta}/2\right) f_{g,\mathrm{EEC}}(x,\theta_a^2) + h_T^{\alpha\beta} d_{g,\mathrm{EEC}}(x,\theta_a^2), \end{aligned} \quad (1)$$

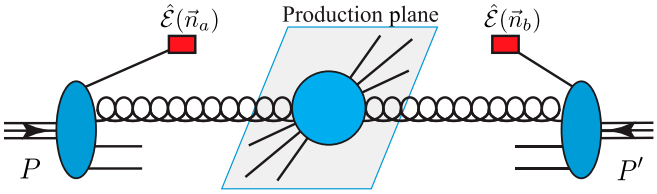

Fig. 1. Nucleon energy–energy correlator measurements in proton–proton collisions at the Large Hadron Collider (LHC). Energy deposits in the forward directions of both incoming hadron beams with polar angles $\theta_{a,b}$ and azimuthal angles $\phi_{a,b}$ represented by $\vec{n}_{a,b}$, respectively.

for the proton moving in the $+\hat{z}$ direction with momentum P, where $\mathcal{F}$ is the gauge field strength tensor and $\mathcal{L}$ is the gauge link. We have kept the azimuthal dependence of the energy flow direction $n_a^\alpha = (1, \sin\theta_a \cos\phi_a, \sin\theta_a \sin\phi_a, \cos\theta_a)$. To parameterize the spinning gluon distribution, we introduce two projection tensors: $g_T^{\alpha\beta} = g^{\alpha\beta} - \left(P^\alpha \overline{n}^\beta + \overline{n}^\alpha P^\beta\right)/\overline{n}\cdot P$ and $h_T^{\alpha\beta} = n_{a,T}^\alpha n_{a,T}^\beta / \left|n_{a,T}^2\right| + g_T^{\alpha\beta}/2$, with $\overline{n}\cdot P = P^0 + P^z \equiv P^+$ and $n_{a,T}^\alpha = (0, \vec{n}_a, 0)$ is the transverse component of n_a^α. These two tensors help to define the normal gluon NEEC $f_{g,\mathrm{EEC}}(x,\theta_a^2)$ and the spinning gluon NEEC $d_{g,\mathrm{EEC}}(x,\theta_a^2)$, respectively. Similarly, we can define the gluon NEECs for the proton moving in the $-\hat{z}$ direction with momentum P' and energy flow direction $n_b^\alpha = (1, \sin\theta_b \cos\phi_b, \sin\theta_b \sin\phi_b, \cos\theta_b)$. The spinning gluon NEEC $d_{g,\mathrm{EEC}}(x,\theta_a^2)$ originates from the interference between different helicity states. To generate a long-range correlation between $\vec{n}_a$ and $\vec{n}_b$, we need to couple two $d_{g,\mathrm{EEC}}(x,\theta^2)$ from both incoming protons, resulting in a $\cos(2\phi)$ asymmetry, where $\phi = \phi_a - \phi_b$.

The spinning gluon distributions of the nucleon have also been studied in the literature under different contexts. In the generalized parton distribution (GPD) framework [41–44], the spinning gluon GPD, also called helicity-flip gluon GPD, predicts a $\cos(2\phi)$ asymmetry in the exclusive processes [45–47]. Meanwhile, in the transverse-momentum-dependent (TMD) formalism, the spinning gluon distribution, referred to as the linearly polarized gluon distribution, leads to a $\cos(2\phi)$ asymmetry in the associated TMD processes [48–55]. More recently, the $\cos(2\phi)$ asymmetry has also been discussed in the context of jet substructures [56–60]. The comparison of these measurements will help us understand the quantum chromodynamics (QCD) associated with the spinning gluon.

Results and Discussion

NEEC for Higgs boson and top quark pair processes at the LHC

The factorization for NEEC in pp collisions is similar to that for deep inelastic scattering processes [7]. As shown in Fig. 1, we measure the energy flows in 2 arbitrary pixels on the calorimeter located at $\vec{n}_a = (\sin\theta_a \cos\phi_a, \sin\theta_a \sin\phi_a, \cos\theta_a)$ and $\vec{n}_b = (\sin\theta_b \cos\phi_b, \sin\theta_b \sin\phi_b, \cos\theta_b)$. The polar angles are measured with respect to the z axis, i.e., the particular rapidities, and the azimuthal angles are measured from the transverse plane perpendicular to the beam direction. We require each of the two pixels to be much closer to one of the hadron beams. Therefore, these two particles are in opposite directions, forward/backward in the lab frame, e.g., $\theta_a \to 0$ and $\theta_b \to \pi$. The generic cross-sectional measurement takes the following form:

$$\Sigma(Q^2;\theta_{a,b},\phi) = \sum_{ij}\int d\sigma(Q^2)\frac{E_i}{E_P}\frac{E_j}{E_P}\mathcal{F}(\phi;\vec{n}_{a,b}) \times\delta(\vec{n}_a - \vec{n}_i)\delta\left(\vec{n}_b - \vec{n}_j\right), \tag{2}$$

where E_P represents the beam energy in pp collisions at the LHC and E_i and E_j represent the energy deposits of particles in $\vec{n}_i$ and $\vec{n}_j$ directions, respectively. $\mathcal{F}(\phi;\vec{n}_{a,b})$ imposes the phase space measurement to construct ϕ. In particular, it measures the polar angles θ_a and θ_b along the beam direction for $\vec{n}_a$ and $\vec{n}_b$, respectively, and the azimuthal angle difference $\phi = \phi_a - \phi_b$, where $\overline{\phi} = (\phi_a + \phi_b)/2$ is integrated out. In the above equation, $d\sigma(Q)$ represents a partonic scattering cross-section. Following previous examples [5], the factorization formula can be written as

$$\begin{aligned}&\Sigma(Q^2;\theta_{a,b},\phi)\\ &= \int d\Omega\Big\{x_a f_{g,\mathrm{EEC}}(x_a,\theta_a^2)x_b f_{g,\mathrm{EEC}}(x_b,\theta_b^2)\widehat{\sigma}_0\\ &+ x_a d_{g,\mathrm{EEC}}(x_a,\theta_a^2)x_b d_{g,\mathrm{EEC}}(x_b,\theta_b^2)\widehat{\sigma}_2(Q^2)\cos(2\phi)\Big\},\end{aligned} \tag{3}$$

where $Q^2 = x_a x_b S_{pp}$, with S_{pp} the center of mass energy squared, and $d\Omega$ represents an additional phase space integral. $\widehat{\sigma}_{0,2}$ are partonic cross-sections calculable perturbatively. Clearly, the $\cos(2\phi)$ azimuthal asymmetry depends on the spinning gluon NEEC $d_{g,\mathrm{EEC}}$ and $\widehat{\sigma}_{0,2}$.

The above factorization argument can follow that of Liu and Zhu [5]. A detailed analysis should be carried out in the future, in particular, for the contributions from the Glauber gluons, whose cancellation plays an important role in the factorization at higher orders.

To study the spinning gluon effect at the LHC, the simplest processes are the Higgs boson production and top quark pair production in pp collisions. We employ perturbative QCD to compute the associated partonic cross-sections $\widehat{\sigma}_{0,2}$; see Eqs. 6 and 7. In Fig. 2, we show the $\cos(2\phi)$ asymmetries, the ratios between the coefficients of $\cos(2\phi)$ and the unpolarized terms in Eq. 3, as functions of rapidity in Higgs boson production and threshold top quark pair production. From this plot, we find that both asymmetries are quite sizable at mid-rapidity, reaching above 50% for both channels. They decrease with rapidity, which reflects the x dependence of the spinning gluon and the normal gluon distributions as described in Eqs. 8 and 9. Experimental measurements of these asymmetries will provide important constraints on the gluon spinning effects.

A similar $\cos(2\phi)$ asymmetry has also been found for Higgs plus two jets' production, where ϕ is the azimuthal angle between the two jets [61]. In common kinematics, the physics behind these two $\cos(2\phi)$ is the same, originating from the spinning gluon. In addition, the positive $\cos(2\phi)$ asymmetry for Higgs boson production is due to its parity. For a CP-odd Higgs, a negative asymmetry would be obtained, similar to those found by Boer et al. [49] and Plehn et al. [61].

For the top quark pair production, as shown in Fig. 3, the $\cos(2\phi)$ asymmetry also depends on the top quark transverse momentum and the rapidity difference between the pair $\Delta y = y_t - y_{\bar{t}}$ with individual rapidities integrated out. Here, the transverse momentum p_T refers to the transverse momentum of an individual quark (or antiquark) in the lab frame, although

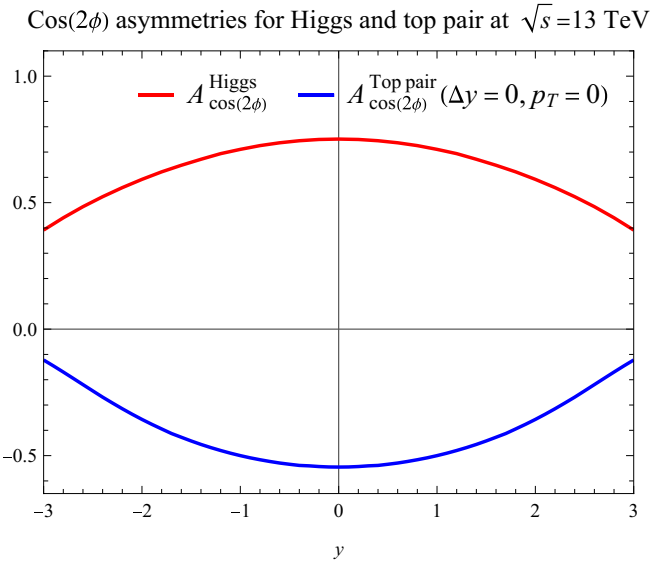

Fig. 2. Long-range cos(2ϕ) azimuthal asymmetries associated with Higgs boson production and top quark pair threshold production as functions of their rapidity y. The asymmetries are computed from the ratios between the coefficients of cos(2ϕ) and the unpolarized terms in Eq. 3 for both channels.

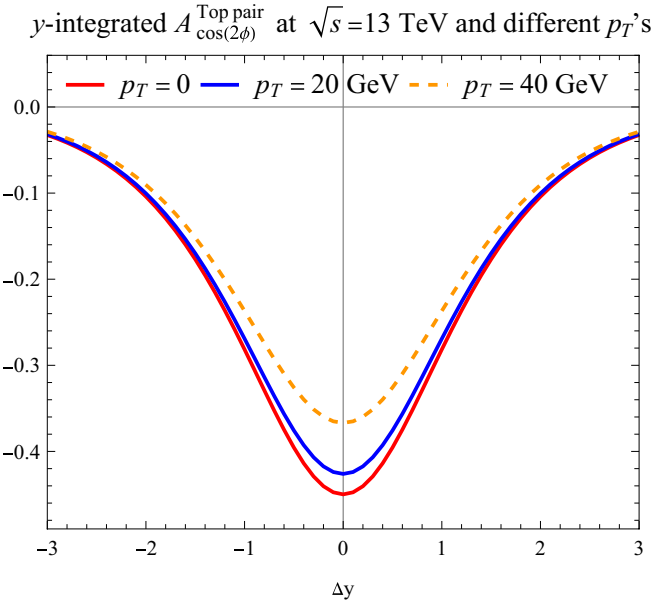

Fig. 3. cos(2ϕ) azimuthal asymmetries in the nucleon energy–energy correlator (NEEC) observable associated with top quark pair production as functions of the rapidity difference between the pair Δy at different p_T values.

their total transverse momentum is zero at this order. We have also computed two-photon production through the gluon–gluon fusion process by applying the amplitudes derived in the literature [62–64], and the cos(2ϕ) asymmetry is smaller as compared to that of Higgs boson production with an opposite sign.

These results demonstrate that the cos(2ϕ) asymmetries can provide a strong case to study the spinning gluon physics at the LHC. More importantly, this shall open a new avenue to study precision physics in the SM. It may also lead to a unique probe of new physics beyond the SM. In particular, the asymmetries crucially depend on the couplings between the gluon fields with different helicities and the Higgs boson, which have been argued to be sensitive to the new physics beyond the SM, and similar studies on TMD-related observables were carried out by Boer et al. [65,66].

Although the above results are based on leading-order calculations, we expect that higher-order corrections will not modify the large cos(2ϕ) asymmetries for the above processes. For example, studies on azimuthal asymmetry between the jets in Higgs plus two jets' production found mild dependence on both higher α_s order corrections [67] and parton showers [68]. Therefore, we anticipate this attribute to persist for an NEEC. In view of the higher-order corrections, we notice that the dominant contributions from soft and collinear gluon radiations have the same behavior for σ_0 and σ_2, in particular for those associated with double logarithms at low transverse momentum of Higgs boson production. Therefore, we expect that our main conclusions will remain the same even at higher orders. Of course, a detailed study is needed for a realistic simulation. We will come back to this issue in a later publication.

Quantum entanglement and test of Bell inequality

The cos(2ϕ) correlation can be interpreted as a signature of entanglement. In an experiment, what is being measured are the real particles that hit the forward detectors. Although these forward-moving particles never come into contact, they remain entangled in their helicities. The physics picture is as follows: Two pairs of entangled real particles and virtual gluons are created through the splitting of the incoming partons. The virtual gluons will participate the partonic hard process, while the real particles will travel toward the forward detectors at opposite ends of the beam with large momentum $E \sim P_z \gg P_t \sim E\theta$. Once the hard process entangles the virtual gluons, it can be demonstrated that the two real particles become entangled instantaneously. In particular, at the time when they are produced, the helicity states of the 2 forward (backward) propagating real partons, p_a and p_b, from the independent splitting processes $\left(p_\alpha \to p_a g_a^*\right.$ and $\left. p_\beta \to p_b g_b^*\right)$ are separable, where p_α and p_β represent the partons before the splitting. However, since the hard interaction will entangle the virtual gluons to have a helicity state of $\left|g_a^* g_b^*\right\rangle \propto |++\rangle + |--\rangle$, it means that if g_a^* is with +-helicity, then g_b^* has also to be in +-helicity. This will in turn force p_a and p_b to be entangled although they never come into interact with each other directly.

This observation provides a basis for testing Bell's theorem [8] through the cos(2ϕ) correlation. Leveraging the NEEC in Eq. 3, one can formulate the Bell observable [69,70]:

$$S(\phi_a,\phi_b) \equiv \frac{\Sigma(\phi_a,\phi_b)+\Sigma(\phi'_a,\phi'_b)-\Sigma(\phi'_a,\phi_b)-\Sigma(\phi_a,\phi'_b)}{\Sigma(\phi_a,\phi_b)+\Sigma(\phi'_a,\phi'_b)+\Sigma(\phi'_a,\phi_b)+\Sigma(\phi_a,\phi'_b)}, \tag{4}$$

where ϕ_a and ϕ_b are azimuthal angles of the energy flow directed toward the detector, measured with respect to arbitrary reference vectors $r_{a,b}$. $\phi' = \phi + \pi/2$ and can be regarded as one measures the azimuthal angles with the reference vectors perpendicular to $r_{a,b}$. For appropriate choices of $\phi_{a,b}$ and $\tilde{\phi}_{a,b}$, the Clauser–Horne–Shimony–Holt (CHSH) inequality [9], an equivalent version of the Bell's original inequality,

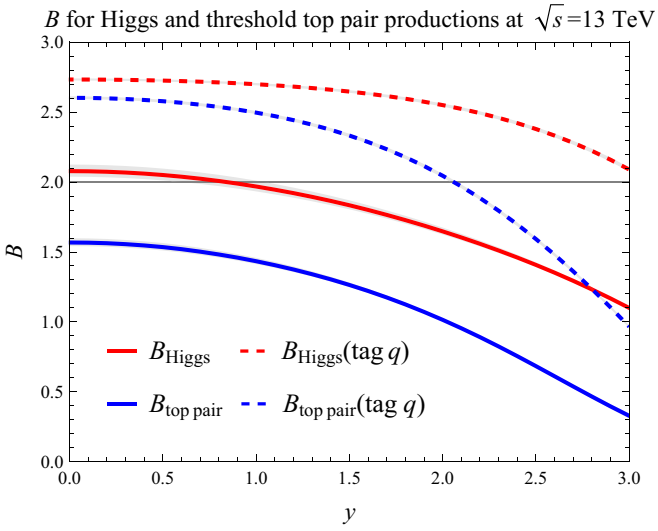

Fig. 4. Violation of the Clauser–Horne–Shimony–Holt (CHSH) inequality in Higgs (red) and top pair (blue) production at the LHC. Quark jet tagging (dashed lines) substantially enhances the significance.

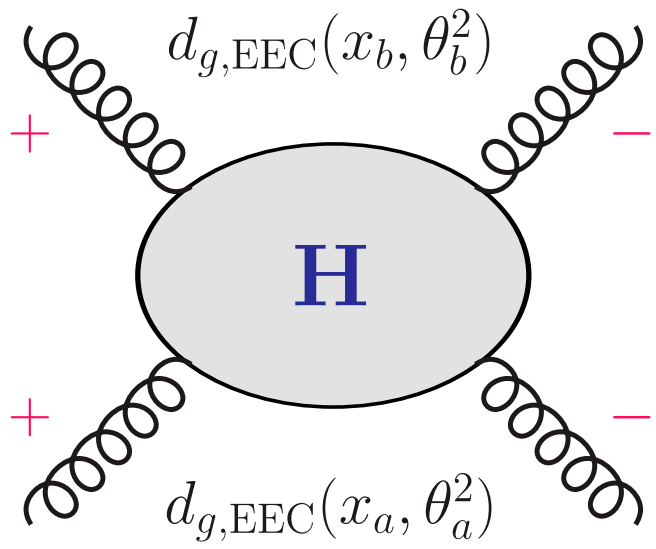

Fig. 5. Long-range $\cos(2\phi)$ asymmetry comes from the interference between double helicity-flip amplitudes in the partonic scattering processes.

$$B \equiv \left| S(\phi_a,\phi_b) - S(\phi_a,\tilde{\phi}_b) + S(\tilde{\phi}_a,\phi_b) + S(\tilde{\phi}_a,\tilde{\phi}_b) \right| \leq 2, \quad (5)$$

can potentially be violated. The maximum violation of the CHSH inequality for any quantum state is given by the Tsirelson's bound, $B_{\max} = 2\sqrt{2} \approx 2.828$ [71]. A proof of Eq. 5 can be found in the Supplementary Materials.

Figure 4 demonstrates the concept by measuring the CHSH inequality in Eq. 5 using the NEEC factorization in Eq. 3. We choose $\phi_a = 0$, $\phi_b = \pi/8$, $\tilde{\phi}_a = \pi/4$, and $\tilde{\phi}_b = 3\pi/8$ [71]. Violation of the CHSH inequality is observed for the Higgs rapidity $y_{\mathrm{Higgs}} < 0.5$. We note that the significance can be dramatically improved by quark jet tagging, meaning that the forward and backward detection of quarks and the NEEC gluon distributions in Eqs. 4 and 5 only receive contributions from the quark splittings, as manifest from Fig. 4, where the CHSH inequality violation is observed for both Higgs and $t\bar{t}$ threshold production. Experimentally, this will be a great challenge and we hope that our results in Fig. 4 will motivate further developments. We also check that increasing the machine energy leads to a more substantial violation, reaching $B \approx 2.36$ for $y_{\mathrm{Higgs}} = 0$ at $\sqrt{S_{pp}} = 33$ TeV without jet tagging, as the entanglement between the detected forward-moving particles intensifies near small x values.

Conclusion

In summary, we studied the long-range azimuthal angular correlations in NEEC measurements in pp collisions at the LHC. For a number of processes, we found substantial large $\cos(2\phi)$ asymmetries. The comparison between these and future studies at the electron–ion collider will provide an important test of the universality of the NEEC distribution functions. Because of the large asymmetries in these processes at the LHC, we emphasize that this will also open a new avenue to study precision physics for the SM, in particular through comparison between Higgs boson production, top quark pair production, and two-photon production. Of course, toward this goal, the backgrounds from other channels are important to explore as well. For example, for Higgs boson production process, there is a weak boson fusion contribution. Although the weak boson fusion contribution is an order of magnitude smaller than the gluon fusion contribution in the total rate, it can potentially dilute the signal. A future study on this should be pursued to solidify the signal.

Although the partonic processes, as those studied in this paper, in general are intrinsically quantum, the quantum entanglement is not always manifest in physical observables. The connection between the $\cos(2\phi)$ correlation and the entanglement makes the long-range correlation in NEEC a promising channel to investigate the quantum entanglement and provide a fundamental test of Bell's inequality. We demonstrate the feasibility of this approach using Higgs and threshold $t\bar{t}$ production at the LHC in which violation of the Bell inequality is substantial when we perform quark jet tagging. Compared to the other collider-based tests discussed in the literature [10–15,17–21,31–33], the long-range correlation in NEEC enables, for the first time, a test of this fundamental quantum property in confined quantities like gluons. Our method benefits from the NEEC factorization theorem, ensuring that the test remains local, thus closing the major potential loophole [32] present in LHC-based tests. Moreover, unlike previous proposals that often require reconstructing the full kinematics, which is usually challenging at the LHC, the NEEC measurement only requires determining the azimuthal angles of the energy flow deposit at the forward detectors, making it more practical for experimental implementation.

Looking ahead, extending this research to other QCD processes, including multijet production, and heavy quarkonium production, will be interesting to follow. Additionally, recent investigations [72–82] have indicated that the quantum entanglement may bring novel perspectives into nuclear and particle physics. We thus anticipate that our work may spark similar endeavors in unraveling the nucleon structures using the quantum information properties. These studies will promise to yield deeper insights into the effects of spinning gluons, complement our current understanding, and potentially reveal new physics beyond the SM.

Methods

To derive the $\cos(2\phi)$ asymmetry in Eq. 3 for the hard processes in pp collisions at the LHC, we apply perturbative QCD to compute the partonic cross-sections $\hat{\sigma}_{0,2}$. In particular, the $\cos(2\phi)$ term $\hat{\sigma}_2$ comes from the interference between double helicity-flip amplitudes where both incoming gluons have the same helicity as illustrated in Fig. 5. In this paper, we focus on the Higgs boson production and top quark pair production processes at the LHC.

For the Higgs boson production process, similar to the TMD case calculated before [48,65,83], the Higgs boson can couple to the spinning gluons directly, and at the leading order

$$\hat{\sigma}_2 = \hat{\sigma}_0 = \pi g_\phi^2 / 64, \tag{6}$$

where g_ϕ represents the coupling between the Higgs boson and the gluon fields in the effective theory $\mathcal{L}_{eff} = -(1/4) g_\phi \Phi F^a_{\mu\nu} F^{a\mu\nu}$ [84]. The above shows that the $\cos(2\phi)$ asymmetry for Higgs production is positive and can reach a sizable value depending on the ratio between $d_{g,\mathrm{EEC}}$ and $f_{g,\mathrm{EEC}}$. On the other hand, for the top quark pair production, $\hat{\sigma}_2$ is different from $\hat{\sigma}_0$,

$$\begin{aligned}
\hat{\sigma}_0 &= \frac{\alpha_s^2 \pi}{\hat{s}^2}\left[\frac{1}{6}\frac{1}{\hat{t}_1\hat{u}_1} - \frac{3}{8}\frac{1}{\hat{s}^2}\right]\left[\hat{t}_1^2 + \hat{u}_1^2 + 4m_t^2\hat{s} - \frac{4m_t^4\hat{s}^2}{\hat{t}_1\hat{u}_1}\right], \\
\hat{\sigma}_2 &= -\frac{\alpha_s^2 \pi}{\hat{s}^2}\left[\frac{1}{6}\frac{1}{\hat{t}_1\hat{u}_1} - \frac{3}{8}\frac{1}{\hat{s}^2}\right]\frac{2m_t^4\hat{s}^2}{\hat{t}_1\hat{u}_1},
\end{aligned} \tag{7}$$

for the dominant $gg \to t\bar{t}$ channel, where $\hat{t}_1 = \hat{t} - m_t^2$ and $\hat{u}_1 = \hat{u} - m_t^2$ and $\hat{s}$, $\hat{t}$, and $\hat{u}$ are the usual Mandelstam variables. In contrast to the Higgs case, the $\cos(2\phi)$ asymmetry for top quark pair production is negative. Interestingly, the asymmetry will reach the maximum value when the pair are close to the threshold where $\hat{s} = 4m_t^2$.

Of course, the final results of $\cos(2\phi)$ asymmetries also depend on the NEEC gluon distributions. When $P^+\theta_a \gg \Lambda_{\mathrm{QCD}}$, they can be computed from perturbative QCD with collinear splitting contributions,

$$\begin{aligned}
f_{g,\mathrm{EEC}}\left(x,\theta_a^2\right) &= \frac{\alpha_s}{2\pi}\frac{1}{\theta_a^2}\int_x^1 \frac{dz}{z}\frac{x(1-z)}{z} \\
&\times\left[\mathcal{P}_{g/q}(z) f_q\left(\frac{x}{z}\right) + \mathcal{P}_{g/g}(z) f_g\left(\frac{x}{z}\right)\right],
\end{aligned} \tag{8}$$

$$\begin{aligned}
d_{g,\mathrm{EEC}}\left(x,\theta_a^2\right) &= \frac{\alpha_s}{2\pi}\frac{1}{\theta_a^2}\int_x^1 \frac{dz}{z}\frac{x(1-z)}{z} \\
&\times\frac{2(1-z)}{z}\left[C_F f_q\left(\frac{x}{z}\right) + C_A f_g\left(\frac{x}{z}\right)\right],
\end{aligned} \tag{9}$$

where $\mathcal{P}_{g/q}$ and $\mathcal{P}_{g/g}$ are the usual collinear splitting kernels. It is interesting to note that the quark splitting contribution to the spinning gluon $d_{g,\mathrm{EEC}}$ leads to the same sign as the gluon splitting one. This is different from the fragmentation case in Chen et al. [56], where there is a cancellation between quark and gluon splitting contributions. Additional Dokshitzer–Gribov–Lipatov–Altarelli–Parisi resummation will modify the power behavior, for which we expect a similar effect for both $f_{g,\mathrm{EEC}}$ and $d_{g,\mathrm{EEC}}$ [56].

Acknowledgments

We thank Meng Xiao for discussions on jet tagging.
Funding: This work is supported by the Natural Science Foundation of China under Contract No. 12175016 (X.L.), the Office of Science of the U.S. Department of Energy under Contract No. DE-AC02-05CH11231 and under the umbrella of the Quark-Gluon Tomography (QGT) Topical Collaboration with Award DE-SC0023646 (Y.G. and F.Y.), the Startup Grant of Peking University, and the Asian Young Scientist Fellowship (H.X.Z.).
Author contributions: All authors contributed to all research steps and writing of the paper.
Competing interests: The authors declare that they have no competing interests.

Data Availability

All data are available in the main text.

Supplementary Materials

Proof of the CHSH inequality in Eq. 9

References

1. Dusling K, Li W, Schenke B. Novel collective phenomena in high-energy proton–proton and proton–nucleus collisions. *Int J Mod Phys E*. 2016;25:1630002.
2. Loizides C. Experimental overview on small collision systems at the LHC. *Nucl Phys A*. 2016;956:200–207.
3. Strickland M. Small system studies: A theory overview. *Nucl Phys A*. 2019;982:92–98.
4. Nagle JL, Zajc WA. Small system collectivity in relativistic hadronic and nuclear collisions. *Ann Rev Nucl Part Sci*. 2018;68:211–235.
5. Liu X, Zhu HX. Nucleon energy correlators. *Phys Rev Lett*. 2023;130:Article 091901.
6. Cao H, Liu X, Zhu HX. Towards the precision nucleon energy-energy correlator in lepton-ion collisions. *Phys Rev D*. 2023;107:Article 114008.
7. Li XL, Liu X, Yuan F, Zhu HX. Illuminating nucleon-gluon interference via calorimetric asymmetry. *Phys Rev D*. 2023;108:Article L091502.
8. Bell JS. On the Einstein Podolsky Rosen paradox. *Phys Physiq Fizika*. 1964;1:195–200.
9. Clauser JF, Horne MA, Shimony A, Holt RA. Proposed experiment to test local hidden-variable theories. *Phys Rev Lett*. 1969;23:880–884.
10. Fabbrichesi M, Floreanini R, Panizzo G. Testing bell inequalities at the LHC with top-quark pairs. *Phys Rev Lett*. 2021;127:Article 161801.
11. Severi C, Boschi CDE, Maltoni F, Sioli M. Quantum tops at the LHC: From entanglement to Bell inequalities. *Eur Phys J C*. 2022;82:Article 285.
12. Barr AJ. Testing Bell inequalities in Higgs boson decays. *Phys Lett B*. 2022;825:Article 136866.
13. Aguilar-Saavedra JA, Casas JA. Improved tests of entanglement and Bell inequalities with LHC tops. *Eur Phys J C*. 2022;82:Article 666.
14. Aguilar-Saavedra JA. Laboratory-frame tests of quantum entanglement in $H \to WW$. *Phys Rev D*. 2023;107(7):Article 076016.

15. Ashby-Pickering R, Barr AJ, Wierzchucka A. Quantum state tomography, entanglement detection and Bell violation prospects in weak decays of massive particles. *J High Energy Phys*. 2023;2023:Article 20.
16. Sinha A, Zahed A. Bell inequalities in 2-2 scattering. *Phys Rev D*. 2023;108:Article 025015.
17. Fabbrichesi M, Floreanini R, Gabrielli E, Marzola L. Bell inequalities and quantum entanglement in weak gauge boson production at the LHC and future colliders. *Eur Phys J C*. 2023;83:Article 823.
18. Aguilar-Saavedra JA. Postdecay quantum entanglement in top pair production. *Phys Rev D*. 2023;108:Article 076025.
19. Bi Q, Cao Q-H, Cheng K, Zhang H. New observables for testing Bell inequalities in W boson pair production. *Phys Rev D*. 2024;109:Article 036022.
20. Han T, Low M, Wu TA. Quantum entanglement and Bell inequality violation in semi-leptonic top decays. *J High Energy Phys*. 2023;2024:Article 192.
21. Ma K, Li T. Testing Bell inequality through $h \to \tau\tau$ at CEPC. *Chin Phys C*. 2023;48(10):Article 103105.
22. Dong Z. When the machine chimes the Bell: Entanglement and Bell inequalities with boosted *tt*. *Phys Rev D*. 2024;109:Article 115023.
23. Morales RA. Exploring Bell inequalities and quantum entanglement in vector boson scattering. *Eur Phys J Plus*. 2023;138:Article 1157.
24. Morales RA. Tripartite entanglement and Bell non-locality in loop-induced Higgs boson decays. *Eur Phys J C*. 2024;84:Article 581.
25. Fabbrichesi M, Floreanini R, Gabrielli E, Marzola L. Bell inequality is violated in $B^0 \to J/\psi K^*(892)^0$ decays. *Phys Rev D*. 2024;109:Article L031104.
26. Fabbrichesi M, Floreanini R, Gabrielli E, Marzola L. Stringent bounds on *HWW* and *HZZ* anomalous couplings with quantum tomography at the LHC. *J High Energy Phys*. 2023;2023:Article 195.
27. Ehatäht K, Fabbrichesi M, Marzola L, Veelken C. Probing entanglement and testing Bell inequality violation with $e^+e^- \to \tau^+\tau^-$ at Belle II. *Phys Rev D*. 2024;109:Article 032005.
28. Fabbrichesi M, Marzola L. Dipole momenta and compositeness of the τ lepton at Belle II. *Phys Rev D*. 2024;109:Article 095026.
29. Fabbrichesi M, Marzola L. Quantum tomography with τ leptons at the FCC-ee: Entanglement, Bell inequality violation, sin θ_W, and anomalous couplings. *Phys Rev D*. 2024;110(7):Article 076004.
30. Kowalska K, Sessolo EM. Entanglement in flavored scalar scattering. *J High Energy Phys*. 2024;2024:Article 156.
31. Bernal A, Caban P, Rembieliński J. Entanglement and Bell inequality violation in vector diboson systems produced in decays of spin-0 particles. arXiv. 2024. https://doi.org/10.48550/arXiv.2405.16525
32. Barr AJ, Fabbrichesi M, Floreanini R, Gabrielli E, Marzola L. Quantum entanglement and Bell inequality violation at colliders. *Prog Part Nucl Phys*. 2024;138:Article 104134.
33. Maltoni F, Severi C, Tentori S, Vryonidou E. Quantum tops at circular lepton colliders. *J High Energy Phys*. 2024;2024:Article 1.
34. ATLAS Collaboration. Observation of quantum entanglement with top quarks at the ATLAS detector. *Nature*. 2024;633:542–547.
35. CMS Collaboration. Observation of quantum entanglement in top quark pair production in proton–proton collisions at $\sqrt{s} =$ 13 TeV. *Rep Prog Phys*. 2024;87(11):Article 117801.
36. CMS Collaboration. Measurements of polarization and spin correlation and observation of entanglement in top quark pairs using lepton+jets events from proton-proton collisions at $\sqrt{s} = 13$ TeV. arXiv. 2024. https://doi.org/10.48550/arXiv.2409.11067
37. Liu H-Y, Liu X, Pan J-C, Yuan F, Zhu HX. Nucleon energy correlators for the color glass condensate. *Phys Rev Lett*. 2023;130:Article 181901.
38. Accardi A, Albacete JL, Anselmino M, Armesto N, Aschenauer EC, Bacchetta A, Boer D, Brooks WK, Burton T, Chang NB, et al. Electron-Ion Collider: The next QCD frontier—Understanding the glue that binds us all. *Eur Phys J A*. 2016;52:Article 268.
39. Abdul Khalek R, Accardi A, Adam J, Adamiak D, Akers W, Albaladejo M, al-bataineh A, Alexeev MG, Ameli F, Antonioli P, et al. Science requirements and detector concepts for the electron-ion collider: EIC yellow report. *Nucl Phys A*. 2022;1026:Article 122447.
40. Prokudin A, Hatta Y, Kovchegov YV, Marquet C, editors. *Proceedings, probing nucleons and nuclei in high energy collisions: Dedicated to the physics of the Electron Ion Collider: Seattle (WA), United States, October 1 – November 16, 2018*. Singapore: World Scientific Publishing; 2020.
41. Ji X. Gauge-invariant decomposition of nucleon spin. *Phys Rev Lett*. 1997;78(4):610–613.
42. Müller D, Robaschik D, Geyer B, Dittes FM, Hořejši J. Wave functions, evolution equations and evolution kernels from light-ray operators of QCD. *Prog Phys*. 1994;42:101–141.
43. Ji X. Deeply virtual Compton scattering. *Phys Rev D*. 1997;55(11):7114–7125.
44. Radyushkin AV. Nonforward parton distributions. *Phys Rev D*. 1997;56(9):5524–5557.
45. Diehl M, Gousset T, Pire B, Ralston JP. Testing the handbag contribution to exclusive virtual Compton scattering. *Phys Lett B*. 1997;411(1–2):193–202.
46. Hoodbhoy P, Ji X. Helicity-flip off-forward parton distributions of the nucleon. *Phys Rev D*. 1998;58(5):Article 054006.
47. Belitsky AV, Müller D. Off-forward gluonometry. *Phys Lett B*. 2000;486(3–4):369–377.
48. Catani S, Grazzini M. QCD transverse-momentum resummation in gluon fusion processes. *Nucl Phys B*. 2011;845(3):297–323.
49. Boer D, Brodsky SJ, Mulders PJ, Pisano C. Direct probes of linearly polarized gluons inside unpolarized hadrons. *Phys Rev Lett*. 2011;106:Article 132001.
50. Metz A, Zhou J. Distribution of linearly polarized gluons inside a large nucleus. *Phys Rev D*. 2011;84:Article 051503.
51. Pisano C, Boer D, Brodsky SJ, Buffing MGA, Mulders PJ. Linear polarization of gluons and photons in unpolarized collider experiments. *J High Energy Phys*. 2013;2013:Article 24.
52. Hatta Y, Xiao B-W, Yuan F, Zhou J. Anisotropy in dijet production in exclusive and inclusive processes. *Phys Rev Lett*. 2021;126:Article 142001.
53. Hatta Y, Xiao B-W, Yuan F, Zhou J. Azimuthal angular asymmetry of soft gluon radiation in jet production. *Phys Rev D*. 2021;104:Article 054037.
54. Esha R, Kang ZB, Lee K, Shao DY, Zhao F. Jet azimuthal anisotropy in *ep* collisions. Paper presented at: DIS2022: XXIX International Workshop on Deep-Inelastic Scattering and Related Subjects; 2022 May 2–6; Santiago de Compostela, Spain. 10.5281/zenodo.7193209.

55. Caucal P, Salazar F, Schenke B, Stebel T, Venugopalan R. Back-to-back inclusive dijets in deep inelastic scattering at small x: Complete NLO results and predictions. *Phys Rev Lett*. 2023;132:Article 081902.
56. Chen H, Moult I, Zhu HX. Quantum interference in jet substructure from spinning gluons. *Phys Rev Lett*. 2021;126:Article 112003.
57. Chen H, Moult I, Zhu HX. Spinning gluons from the QCD light-ray OPE. *J High Energy Phys*. 2022;8:Article 233.
58. Karlberg A, Salam GP, Scyboz L, Verheyen R. Spin correlations in final-state parton showers and jet observables. *Eur Phys J C*. 2021;81:Article 681.
59. Yu Z, Yuan CP. Azimuthal angular correlation as a boosted top jet substructure. *Phys Rev Lett*. 2022;129:Article 112001.
60. Yu Z, Mohan KA, Yuan CP. Determining the CP property of $ht\bar{t}$ coupling via a novel jet substructure observable. *Phys Lett B*. 2024;856:Article 138959.
61. Plehn T, Rainwater DL, Zeppenfeld D. Determining the structure of Higgs couplings at the CERN large hadron collider. *Phys Rev Lett*. 2002;88(5):Article 051801.
62. Dicus DA, Willenbrock SSD. Photon pair production and the intermediate-mass Higgs boson. *Phys Rev D*. 1988;37(7): 1801–1809.
63. Bern Z, De Freitas, Dixon LJ. Two-loop amplitudes for gluon fusion into two photons. *J High Energy Phys*. 2001;2001:037.
64. Qiu J-W, Schlegel M, Vogelsang W. Probing gluonic spin-orbit correlations in photon pair production. *Phys Rev Lett*. 2011;107(6):Article 062001.
65. Boer D, den Dunnen, Pisano C, Schlegel M, Vogelsang W. Linearly polarized gluons and the Higgs transverse momentum distribution. *Phys Rev Lett*. 2012;108:Article 032002.
66. Boer D, den Dunnen, Pisano C, Schlegel M. Determining the Higgs spin and parity in the diphoton decay channel. *Phys Rev Lett*. 2013;111:Article 032002.
67. Campbell JM, Ellis RK, Zanderighi G. Next-to-leading order Higgs + 2 jet production via gluon fusion. *J High Energy Phys*. 2006;2006:028.
68. Del Duca, Klämke G, Mangano ML, Moretti M, Piccinini F, Pittau R, Polosa AD, Zeppenfeld D. Monte Carlo studies of the jet activity in Higgs + 2 jet events. *J High Energy Phys*. 2006;2006:016.
69. Leach J, Jack B, Romero J, Ritsch-Marte M, Boyd RW, Jha AK, Barnett SM, Franke-Arnold S, Padgett MJ. Violation of a Bell inequality in two-dimensional orbital angular momentum state-spaces. *Opt Express*. 2009;17(10):8287–8293.
70. Zhang D, Qiu X, Zhang W, Chen L. Violation of a Bell inequality in two-dimensional state spaces for radial quantum number. *Phys Rev A*. 2018;98:Article 042134.
71. Cirelson BS. Quantum generalizations of Bell's inequality. *Lett Math Phys*. 1980;4:93–100.
72. Kharzeev DE, Levin EM. Deep inelastic scattering as a probe of entanglement. *Phys Rev D*. 2017;95:Article 114008.
73. Beane SR, Kaplan DB, Klco N, Savage MJ. Entanglement suppression and emergent symmetries of strong interactions. *Phys Rev Lett*. 2019;122:Article 102001.
74. Tu Z, Kharzeev DE, Ullrich T. Einstein-Podolsky-Rosen paradox and quantum entanglement at subnucleonic scales. *Phys Rev Lett*. 2020;124:Article 062001.
75. Mueller N, Tarasov A, Venugopalan R. Deeply inelastic scattering structure functions on a hybrid quantum computer. *Phys Rev D*. 2020;102:Article 016007.
76. Gong W, Parida G, Tu Z, Venugopalan R. Measurement of Bell-type inequalities and quantum entanglement from Λ-hyperon spin correlations at high energy colliders. *Phys Rev D*. 2022;106:Article L031501.
77. Armesto N, Dominguez F, Kovner A, Lublinsky M, Skokov V. The color glass condensate density matrix: Lindblad evolution, entanglement entropy and Wigner functional. *J High Energy Phys*. 2019;2019:–25.
78. Kharzeev DE. Quantum information approach to high energy interactions. *Phil Trans A Math Phys Eng Sci*. 2021;380:20210063.
79. Low I, Mehen T. Symmetry from entanglement suppression. *Phys Rev D*. 2021;104:Article 074014.
80. Carena M, Low I, Wagner CEM, Xiao M-L. Entanglement suppression, enhanced symmetry, and a standard-model-like Higgs boson. *Phys Rev D*. 2024;109:Article L051901.
81. Sakurai K, Spannowsky M. Three-body entanglement in particle decays. *Phys Rev Lett*. 2024;132:Article 151602.
82. Hentschinski M, Kharzeev DE, Kutak K, Tu Z. Probing the onset of maximal entanglement inside the proton in diffractive deep inelastic scattering. *Phys Rev Lett*. 2023;131:Article 241901.
83. Sun P, Xiao B-W, Yuan F. Gluon distribution functions and Higgs boson production at moderate transverse momentum. *Phys Rev D*. 2011;84:Article 094005.
84. Dawson S. Radiative corrections to Higgs boson production. *Nucl Phys B*. 1991;359(2–3):283–300.